NASA TECHNICAL MEMORANDUM

NASA TM X-1857

NASA TM X-1857

THE CALCULATED RESPONSE OF A THREE-CRYSTAL PAIR SPECTROMETER

by Clemans A. Powell, Jr.

Langley Research Center

Langley Station, Hampton, Va.

NATIONAL AERONAUTICS AND SPACE ADMINISTRATION • WASHINGTON, D. C. • AUGUST 1969

1. Report No. NASA TM X-1857	2. Government Accession No.	3. Recipient's Catalog No.
4. Title and Subtitle THE CALCULATED RESPONSE OF A THREE-CRYSTAL PAIR SPECTROMETER		5. Report Date August 1969 6. Performing Organization Code
7. Author(s) Clemans A. Powell, Jr.		8. Performing Organization Report No. L-6672
9. Performing Organization Name and Address NASA Langley Research Center Hampton, Va. 23365		10. Work Unit No. 124-09-11-03-23 11. Contract or Grant No.
12. Sponsoring Agency Name and Address National Aeronautics and Space Administration Washington, D.C. 20546		13. Type of Report and Period Covered Technical Memorandum 14. Sponsoring Agency Code

15. Supplementary Notes

16. Abstract

A computer analysis has been made to determine the response and efficiency of a three-crystal sodium iodide scintillation spectrometer. An iterative spectrum-unfolding method has been modified to analyze experimental spectra taken with the spectrometer. The response and efficiency agree well with limited experimental data. The unfolding technique yields errors in response and efficiency much smaller than those anticipated.

17. Key Words Suggested by Author(s)	18. Distribution Statement
Photon spectrometer Three-crystal coincidence spectrometer Sodium iodide Pair spectrometer	Unclassified – Unlimited

19. Security Classif. (of this report)	20. Security Classif. (of this page)	21. No. of Pages	22. Price*
Unclassified	Unclassified	35	$3.00

*For sale by the Clearinghouse for Federal Scientific and Technical Information
Springfield, Virginia 22151

THE CALCULATED RESPONSE OF A THREE-CRYSTAL PAIR SPECTROMETER

By Clemans A. Powell, Jr.
Langley Research Center

SUMMARY

An investigation has been made of the use of a three-crystal sodium iodide pair spectrometer for the quantitative measurement of photon spectra over an energy range from 1.5 MeV to 10.0 MeV. The investigation included developing a computer analysis of the response and efficiency of the detector system and using an iterative unfolding method to analyze pulse-height distributions obtained with the system. The efficiency analysis considers the specific geometry of the three crystals and the attenuation of photons in the housings and reflectors of the assemblies. Simplifying assumptions used are as follows: (1) The pair-production processes of the incident photons occur on the central axis of the center crystal and (2) the resulting electron-positron pairs are brought to rest at their point of creation. The response of the spectrometer to monoenergetic photon sources was determined by using the efficiency calculations and the experimentally measured response to a known source. The iterative unfolding method uses these calculated responses to obtain experimental photon spectra from pulse-height distributions.

The predicted efficiencies agree well with experimental efficiencies measured from an americium-beryllium source. The unfolding procedure has been tested by using simulated spectra and has proved to yield errors much smaller than the errors introduced by either the predicted efficiencies or responses.

INTRODUCTION

For many years the sodium iodide (NaI) scintillation detector has been the basis of various forms of spectrometers for measurements of gamma rays, characteristic X-rays, and bremsstrahlung. Among these forms are simple, single-crystal detectors; cylindrical crystal detectors with anticoincidence annuli; two crystals in coincidence; and three crystals in coincidence. All the latter forms are designed to overcome one of the major shortcomings of the simple, single-crystal detectors. Because of Compton scattering and losses of pair-production annihilation quanta, the response in the form of pulse-height distributions from a single-crystal spectrometer is quite complicated, especially when measuring energies above 2 MeV. However, the three-crystal spectrometer is capable of

distinguishing between pair-production processes and the other forms of interaction of photons with the scintillation material and yields pulse-height distributions with single peaks for monoenergetic photons. Some previous uses of such a spectrometer are reported in references 1, 2, and 3.

Before any type of spectrometer can be used in a quantitative experiment, the response of the spectrometer must be known over the photon-energy range of interest. Because there are only a small number of readily available sources of known photon energy above 1.5 MeV (the lower limit of the spectrometer's usefulness), a means of theoretically predicting the response of the spectrometer is necessary. In addition, some means of unfolding or analyzing the experimental pulse-height distributions is necessary to yield meaningful experimental spectra. The present effort was made to furnish the needed information.

Theoretical predictions have been made of the efficiency of a three-crystal pair spectrometer and its response to a range of monoenergetic photons, and an iterative method has been found to unfold the experimental pulse-height distributions. Not all entering photons are sensed by the spectrometer, and the efficiency analysis evaluates the effect of the geometry of the three crystals and the attenuation losses of photons in the reflectors and housings of the detector assemblies. The response of the spectrometer to a range of monoenergetic photons has been determined from the calculated efficiencies and the shape of an experimental spectrum of a known monoenergetic source. The unfolding method is based on an iterative procedure developed in reference 4.

SYMBOLS

$\underline{B}$ response matrix for spectrometer

B element of $\underline{B}$

$\underline{C}$ matrix defined by $\underline{C} = \tilde{\underline{B}}\underline{B}$

$\underline{D}$ diagonal matrix; $\underline{N} = \underline{D}\underline{S}$

D element of $\underline{D}$

d distance along ζ-axis from point of annihilation-quanta creation to origin of η,ζ,ξ coordinate system, cm

E photon energy, MeV

F	peak-to-total interaction ratio (photofraction) for side detectors
H	height of side crystals, cm
I	indentation of center detector into well bounded by side detectors, cm
i,j,k	increment numbers for t, θ, and φ, respectively
L	length of center detector, cm
$\underline{M}$	matrix of pulse-height distribution
M	element of $\underline{M}$
$\underline{N}$	matrix of photon-energy spectrum
N	element of $\underline{N}$
m,n,p	indices of matrix elements
P	probabilities of interactions making up resultant efficiency of spectrometer
q	distance from point of annihilation-quanta creation to outer surface of side detectors, cm
R	radius of detector, cm
r	distance from point of pair production on Z-axis to surface of center crystal, cm
$\underline{S}$	matrix defined by $\underline{S} = \underline{\tilde{B}}\,\underline{M}$
S	element of $\underline{S}$
T	sum of squares of difference in S_p and its iterative approximation
t	distance of point of pair production from origin along Z-axis, cm
u	maximum value of m

v	maximum value of n
X,Y,Z	coordinate system with origin at center of front face of center detector
X',Y'	floating coordinate system with origin at point of annihilation-quanta production
x	detector light shield thickness, cm
x'	annihilation-quanta path length through light shield, cm
y	reflector material thickness, cm
y'	annihilation-quanta path length through reflector material, cm
α	total number of increments
$\Delta\Omega$	incremental solid angle
$\Delta\theta,\Delta\varphi$	incremental polar angles
Δt	increment of center detector thickness, cm
η,ζ,ξ	coordinate system with origin at center of end face of side detector
θ,φ	polar angles from point of annihilation-quanta production, rad
θ'	polar angle measured from ξ-axis to a point on surface of side detectors, rad
μ	mass attenuation coefficient, cm^{-1}
ρ	radius of hemicylindrical groove in face of side detector, cm
τ	distance from origin of η,ζ,ξ coordinate system to a point on surface of side detectors, cm

Subscripts:

a	aluminum

c	center detector
e	total attenuation for NaI
f	stainless steel
g	pair-production attenuation for NaI
i,j,k	indices for increments of t, θ, and φ, respectively
m,n,p	indices of matrix elements
r	reflector material Al_2O_3
s	side detector
t	thickness of center detector
u	maximum value of m
v	maximum value of n
θ,φ	polar angles
1,2	identification numbers of annihilation quanta

Superscripts:

q	iteration number
1	first iterative approximation

A tilde (~) over the symbol for a matrix indicates the transpose of that matrix.

SPECTROMETER OPERATION

A sketch of the detector described in the present report is shown in figure 1. The spectrometer consists of a center NaI scintillation detector, 4.12 cm in diameter and 10.16 cm long, which is coupled to a photomultiplier tube inside a magnetic-shielded

housing. In addition, there are two NaI annihilation detectors. Each detector is 12.70 cm in diameter and 7.62 cm in height and has a photomultiplier tube and a magnetic shield with a hemicylindrical slot of 2.54-cm radius machined across the end face. During operation, the two side detectors are placed face to face, and the center detector is placed in the cylindrical well formed by the grooves in the side detectors.

Photons incident on the center detector interact with the scintillation material (NaI activated with thallium) by three distinct processes: photoelectric effect, Compton scattering, and, if greater than 1.022 MeV, pair production. It is assumed that if a pair-production process occurs, the resulting electron-positron pair deposits its energy in the detector and is brought to rest. The positron combines with an electron in the detector, and the pair promptly annihilates, emitting two photons of equal energy (0.511 MeV) in opposite directions. If these photons escape being captured by the center detector and are captured by the side detectors, the events are recorded. Figure 2 shows a block diagram of the electronics used to insure that the necessary coincidences are met and to analyze the resultant spectra. The light output from the scintillation detectors is proportional to the energy deposited in each detector; consequently, if a pair-production process occurs in the center detector, the light output and electrical pulse from the center detector are proportional to $E - 1.022$, where E is the incident photon energy in MeV. In order to insure that the pulses recorded in the center detector were produced by a pair-production process, pulses from the center detector were recorded only when 0.511-MeV pulses were registered in each of the side detectors. The single-channel analyzers, coincidence unit, and linear gate unit insure that only the proper pulses are recorded.

The greatest benefit of a three-crystal spectrometer is the simplicity of the spectrum produced by monoenergetic photons. Figure 3 shows the spectra produced in both a 7.62-cm by 7.62-cm single-crystal NaI detector and the present three-crystal spectrometer by the 4.43-MeV gamma ray from the $^{9}Be(\alpha,n\gamma)^{12}C$ reaction. The single-crystal spectrum exhibits a complicated structure with three distinct peaks, corresponding to the full-energy peak and two escape peaks resulting from the escape of either or both of the pair-production annihilation quanta. There are a number of counts recorded in the lower channels because of losses from Compton scattered photons. The three-crystal spectrometer spectrum, on the other hand, has a much simpler shape and is essentially a Gaussian peak plus a low-energy tail. This low-energy tail is the result of bremsstrahlung losses and electron escape from the center detector.

The primary disadvantages of a three-crystal pair spectrometer are low efficiency and because of the minimum energy necessary for the creation of the electron-positron pairs, a relatively high lower limit of photon-energy sensitivity. The rest mass energy of an electron-positron pair is 1.022 MeV, but the useful lower limit of photon-energy

sensitivity is approximately 1.5 MeV for such a spectrometer because the pair-production cross section is extremely small at the lower energies. In order to obtain quantitative results from the use of a spectrometer as described in this report, whether it is used for measuring the spectra of discrete energy photons or continuous spectra as in the case of bremsstrahlung, it is necessary to know the efficiency and response of the spectrometer to monoenergetic photons over the energy range of interest. In addition, for continuous spectra or for spectra of many monoenergetic photons, a means of analyzing the experimentally determined pulse-height distributions must be found.

CALCULATION OF SPECTROMETER EFFICIENCY

The efficiency of a three-crystal pair spectrometer is dependent on the specific geometry of the three detectors. Figure 4 gives the basic geometry of the detectors and the coordinate system on which the following discussions depend. This coordinate system has the origin at the center of the front face of the center detector and the Z-axis along the central axis of the center detector.

In computing the efficiency of the system, the following processes are considered in turn, and the resulting efficiency is the product of the probability of the occurrence of each of them:

(1) Passage of photons through the light shield and reflector of the center detector

(2) Pair production at various points in the center detector

(3) Capture of the annihilation quanta in the center detector and its light shield and reflector

(4) Capture of the annihilation quanta in the light shields and reflectors of the side detectors

(5) Capture of the annihilation quanta in the side detectors

The resulting efficiency of the system will be shown to be of the following form:

$$P[E] = P[\text{entrance}] \sum_i P_i[\text{pair production}] \sum_j \sum_k \left\{ P_{j,k}[\Delta\Omega]\, P_{j,k}[\text{escape}]\, P_{j,k}[\text{pair capture}] \right\}$$

where $P[\text{entrance}]$ is the probability that a photon will pass through the light shield and reflector of the center detector, $P_i[\text{pair production}]$ is the probability that a pair-production event will occur at some position in the center crystal as determined by the indexing integer i, $P_{j,k}[\Delta\Omega]$ is the probability that the annihilation quanta will be emitted in directions determined by the indexing integers j and k, $P_{j,k}[\text{escape}]$ is

the probability that the annihilation quanta will escape being captured in the center crystal, and $P_{j,k}[\text{pair capture}]$ is the probability that the pairs will be captured in the side detectors.

Processes in Center Detector

Gamma rays or photons impinging on the center detector from the negative Z-direction will be attenuated by the wall and reflector material surrounding the center NaI crystal. The material (not shown in fig. 4) used on the end window of the present detector is 0.04 cm of aluminum, and the reflector is 0.28 cm of powdered aluminum oxide (Al_2O_3). The probability of a photon entering the center NaI crystal is

$$P[\text{entrance}] = \exp\left[-(\mu_a x_c + \mu_r y_c)\right] \tag{1}$$

where μ_a and μ_r are the attenuation coefficients for aluminum and the reflector material, respectively; and x_c and y_c are the respective wall thickness and reflector thickness of the center detector.

All photons which interact with the center detector are assumed to enter and interact along the central Z-axis. This is a reasonable assumption, since, under operating conditions, a collimator is used to confine the incident beam to an area much smaller than the cross-sectional area of the detector. The point of interaction is the intersection of X' and Y', a distance t from the intersection of X and Y. If the displacement t is incremented into a number α_t of thicknesses Δt, then

$$t = i\,\Delta t \qquad (i = 1,2,3, \ldots \alpha_t) \tag{2}$$

The probability of having a pair-production process in the ith thickness increment is given by

$$P_i[\text{pair production}] = \exp\left[-\mu_e(i-1)\Delta t\right]\left\{1 - \exp\left[-\mu_g \Delta t\right]\right\} \tag{3}$$

where μ_e and μ_g are the respective total and pair-production interaction (or attenuation) coefficients for sodium iodide. Pairs produced by Compton scattered photons are neglected.

It is further assumed that the electron-positron pairs are stopped within the ith increment of their creation and that annihilation occurs in the same increment along the Z-axis. By assuming that the velocity vectors of the annihilation quanta created are uniformly distributed, the probability of one of the gammas of a pair being emitted into an incremental solid angle $\Delta\Omega$ with direction θ,φ and the other with direction $\theta + \pi$,

$\varphi + \pi$ is

$$P_{j,k}[\Delta\Omega] \approx \frac{1}{4\pi} \sin(j\ \Delta\theta)\Delta\theta\ \Delta\varphi \tag{4}$$

where

$$\theta = j\ \Delta\theta \qquad \left(j = 0,1,2, \ldots \alpha_\theta;\ \ \Delta\theta = \frac{\pi}{\alpha_\theta}\right)$$

$$\varphi = k\ \Delta\varphi - \frac{\pi}{2} \qquad \left(k = 0,1,2, \ldots \alpha_\varphi;\ \ \Delta\varphi = \frac{2\pi}{\alpha_\varphi}\right)$$

Some of the quanta emitted from the ith thickness increment will be captured in the center detector. The probability that both annihilation quanta will escape from the center detector and its light shield and reflector is

$$P_{j,k}[\text{escape}] = \exp\left[-\mu_e\left(r_{c,1} + r_{c,2}\right) - \mu_a\left(x'_{c,1} + x'_{c,2}\right) - \mu_r\left(y'_{c,1} + y'_{c,2}\right)\right] \tag{5}$$

where $r_{c,1}$ and $r_{c,2}$ are the respective distances from the point of pair production on the Z-axis to the surface of the center NaI crystal, $x'_{c,1}$ and $x'_{c,2}$ are the respective thicknesses of wall material traversed, and $y'_{c,1}$ and $y'_{c,2}$ are the respective thicknesses of reflector material traversed for the annihilation quanta 1 and 2. These thicknesses are dependent on the angle θ for the emission of the annihilation quanta. This dependence is summarized in the following relationships:

If $\theta < \frac{\pi}{2}$,

$$\left.\begin{aligned} r_{c,1} &= \frac{R_c}{\sin\theta} \\ x'_{c,1} &= \frac{x_c}{\sin\theta} \\ y'_{c,1} &= \frac{y_c}{\sin\theta} \end{aligned}\right\} \quad \text{for} \quad \tan\theta \geqq \frac{R_c}{L - t} \tag{6a}$$

$$\left.\begin{aligned} r_{c,2} &= \left|\frac{R_c}{\sin(\theta+\pi)}\right| = \frac{R_c}{\sin\theta} \\ x'_{c,2} &= \left|\frac{x_c}{\sin(\theta+\pi)}\right| = \frac{x_c}{\sin\theta} \\ y'_{c,2} &= \left|\frac{y_c}{\sin(\theta+\pi)}\right| = \frac{y_c}{\sin\theta} \end{aligned}\right\} \quad \text{for} \quad \tan(\theta+\pi) \geqq \frac{R_c}{t} \quad \text{or} \quad \tan(\theta) \geqq \frac{R_c}{t} \tag{6b}$$

$$\left.\begin{aligned} r_{c,2} &= \left|\frac{t}{\cos(\theta+\pi)}\right| = \frac{t}{\cos\theta} \\ x'_{c,2} &= \left|\frac{x_c}{\cos(\theta+\pi)}\right| = \frac{x_c}{\cos\theta} \\ y'_{c,2} &= \left|\frac{y_c}{\cos(\theta+\pi)}\right| = \frac{y_c}{\cos\theta} \end{aligned}\right\} \quad \text{for} \quad \tan(\theta+\pi) = \tan\theta < \frac{R_c}{t} \tag{6c}$$

If $\theta \geqq \frac{\pi}{2}$,

$$\left.\begin{aligned} r_{c,1} &= \frac{R_c}{\sin\theta} \\ x'_{c,1} &= \frac{x_c}{\sin\theta} \\ y'_{c,1} &= \frac{y_c}{\sin\theta} \end{aligned}\right\} \quad \text{for} \quad \left|\tan\theta\right| = -\tan\theta > \frac{R_c}{t} \tag{6d}$$

$$\left.\begin{aligned} r_{c,1} &= \left|\frac{t}{\cos\theta}\right| = -\frac{t}{\cos\theta} \\ x'_{c,1} &= \left|\frac{x_c}{\cos\theta}\right| = -\frac{x_c}{\cos\theta} \\ y'_{c,1} &= \left|\frac{y_c}{\cos\theta}\right| = -\frac{y_c}{\cos\theta} \end{aligned}\right\} \quad \text{for} \quad \left|\tan\theta\right| = -\tan\theta \leqq \frac{R_c}{t} \tag{6e}$$

$$\left.\begin{aligned} r_{c,2} &= \left|\frac{R_c}{\sin(\theta+\pi)}\right| = \frac{R_c}{\sin\theta} \\ x'_{c,2} &= \left|\frac{x_c}{\sin(\theta+\pi)}\right| = \frac{x_c}{\sin\theta} \\ y'_{c,2} &= \left|\frac{y_c}{\sin(\theta+\pi)}\right| = \frac{y_c}{\sin\theta} \end{aligned}\right\} \quad \text{for} \quad \left|\tan(\theta+\pi)\right| = -\tan\theta \geq \frac{R_c}{L-t} \tag{6f}$$

where L is the length and R_c is the radius of the center NaI detector. If $\theta < \frac{\pi}{2}$ and $\tan\theta < \frac{R_c}{L-t}$, annihilation quantum 1 will escape from the center crystal through the photomultiplier tube and has no chance of being captured by the side detectors. Similarly, if $\theta > \frac{\pi}{2}$ and $\left|\tan(\theta+\pi)\right| = -\tan(\theta) < \frac{R_c}{L-t}$, annihilation quantum 2 will escape being captured by one of the side detectors. In either of these cases, the probability of capturing both annihilation quanta with the side detectors is zero.

Processes in Annihilation-Quanta Detectors

If both quanta of a pair are able to escape from the center detector and its housing, the probability that one, or both, will interact with the side detectors can be predicted by considering the direction of emission, the attenuation by the housing and reflector of the side detector, and the interaction of the quanta with the NaI crystals. If a quantum (for example, quantum 1) enters one of the NaI side detectors, the probability that it will interact with the crystal is

$$P_{j,k}[\text{interaction of } 1] = 1 - \exp\left[-\mu_e r_{s,1}\right] \tag{7}$$

where $r_{s,1}$ is the distance that a quantum traverses through a side detector along a path with origin at $0'$. This distance is given by

$$r_{s,1} = q_1 - \frac{\rho}{\sin\theta} \tag{8}$$

where q_1 is the total distance from $0'$ to a point on the surface of the side detector as determined by θ and φ, and ρ is the radius of the hemicylindrical groove cut into the face of the detector. The same relations hold if φ is such that annihilation quantum 1 passes through the other side detector. Because of this symmetry about the Y-Z plane, the remaining discussions will assume that annihilation quantum 1 is emitted only when

$-\frac{\pi}{2} \leqq \varphi \leqq \frac{\pi}{2}$, and in the final summation over φ the resulting probability will be multiplied by two. Similarly, the probability that the other annihilation quantum will interact with the NaI crystal of the other side detector is given by

$$P_{j,k}[\text{interaction of } 2] = 1 - \exp\left[-\mu_e r_{s,2}\right] \tag{9}$$

where $r_{s,2}$ is the distance that annihilation quantum 2 traverses through the crystal along a path with origin at $0'$ and is given by

$$r_{s,2} = q_2 + \frac{\rho}{\sin(\theta + \pi)} = q_2 - \frac{\rho}{\sin \theta} \tag{10}$$

where q_2 is the total distance from $0'$ on the Z-axis of the center detector to a point on the surface of the side detector as determined by θ and φ.

The following discussion of determining the distances q_1 and q_2 is more easily visualized by redefining the coordinate system for the side detectors as shown in figure 5. For simplicity the grooves in the face of the detector are omitted. The ζ-axis is along the Z-axis in figure 4. If θ and φ are such that annihilation quantum 1 exits through the flat face of the upper crystal as in figure 5(a),

$$\cot \theta' = \cot \theta + \frac{d}{H} \cos \varphi \tag{11}$$

where d is the distance of the point of annihilation pair production on the ζ-axis from the origin, and H is the crystal height. The position d is given in terms of the original X,Y,Z coordinate system by

$$d = (I + t) - R_S \tag{12}$$

where I is the indentation of the center detector into the side detectors, R_S is the radius of the side detectors, and t is as defined in figure 4.

On the face of the crystal,

$$\eta^2 + \zeta^2 \leqq R_S^2 \tag{13}$$

where

$$\eta = \tau_1 \sin \theta' \sin \varphi$$

$$\zeta = \tau_1 \cos \theta'$$

Also,

$$\tau_1 = \frac{H}{\sin \theta' \cos \varphi}$$

or by substitution,

$$H^2 \tan^2 \varphi + H^2 \frac{\cot^2 \theta'}{\cos^2 \varphi} \leq R_s^2 \tag{14}$$

By substituting equation (11) for $\cot \theta'$ into equation (14), the necessary condition for the quantum to exit through the face of the side crystal is given by

$$H^2 \left[\tan^2 \varphi + \frac{\left(\cot \theta + \frac{d}{H} \cos \varphi \right)^2}{\cos^2 \varphi} \right] \leq R_s^2 \tag{15}$$

If this relation holds for a particular value of θ and φ, then q_1 is given by

$$q_1 = \frac{H}{\sin \theta \cos \varphi} \tag{16}$$

Because of the symmetry about the $\eta - \zeta$ plane, the necessary condition for the other quantum to exit through the end face of the other crystal is given by

$$H^2 \left[\tan^2 \varphi + \frac{\left(\cot \theta - \frac{d}{H} \cos \varphi \right)^2}{\cos^2 \varphi} \right] \leq R_s^2 \tag{17}$$

If the condition of equation (17) is met, then

$$q_2 = \frac{H}{\sin \theta \cos \varphi} \tag{18}$$

If either condition (16) or (18) is not met, one or both of the annihilation quanta will exit through the side of the crystal; and the distances from the point of creation through either crystal can be found by using figure 5(b) and the relation

$$\tau_1^2 = R_s^2 + \xi^2 \tag{19}$$

where

$$\xi = q_1 \sin\theta \cos\varphi$$

and

$$\tau_1 = q_1 \frac{\sin\theta}{\sin\theta'}$$

From the triangle formed by the sides d, q_1, and τ_1, it can be shown that

$$\cot\theta' = \cot\theta + \frac{d}{q_1 \sin\theta} \tag{20a}$$

and squaring yields

$$\cot^2\theta' = \cot^2\theta + \frac{2d}{q_1}\frac{\cos\theta}{\sin^2\theta} + \frac{d^2}{q_1^2\sin^2\theta} \tag{20b}$$

From equation (19) it can be found that

$$\csc^2\theta' = \frac{R_s^2}{q_1^2\sin^2\theta} + \cos^2\varphi \tag{21}$$

By using the trigonometric relationship, $\csc^2\theta' = 1 + \cot^2\theta'$, equations (20) and (21) can be combined to yield

$$1 + \cot^2\theta + \frac{2d}{q_1}\frac{\cos\theta}{\sin^2\theta} + \frac{d^2}{q_1^2\sin^2\theta} = \frac{R_s^2}{q_1^2\sin^2\theta} + \cos^2\varphi \tag{22}$$

or upon rearranging

$$q_1^2\left(1 - \sin^2\theta\cos^2\varphi\right) + 2q_1 d\cos\theta + \left(d^2 - R_s^2\right) = 0$$

or solving for q_1

$$q_1 = \frac{-d\cos\theta + \sqrt{d^2\cos^2\theta + \left(R_s^2 - d^2\right)\left(1 - \sin^2\theta\cos^2\varphi\right)}}{\left(1 - \sin^2\theta\cos^2\varphi\right)} \tag{23}$$

The positive radical is used because q_1 cannot be negative.

Again by using the previous symmetry arguments, q_2 can be found to be

$$q_2 = \frac{d \cos\theta + \sqrt{d^2\cos^2\theta + \left(R_S^2 - d^2\right)\left(1 - \sin^2\theta \cos^2\varphi\right)}}{\left(1 - \sin^2\theta \cos^2\varphi\right)} \tag{24}$$

Under actual operating conditions the single-channel analyzers connected to the side detectors have their lower levels and window widths adjusted to accept only pulses with amplitudes within the width of the full-energy peak for the 0.511-MeV photons. This requirement makes certain that only pair-production processes are analyzed; that is, Compton scattered photons from the center detector probably will not be able to trigger the coincidence unit. Therefore, the interaction probability for the side detectors must be multiplied by the peak-to-total counting ratio (called photofraction) for the particular detectors used. Theoretical data presented in reference 5 indicate that for NaI detectors with diameters from 7.6 cm to 12.7 cm and heights from 7.6 cm to 12.7 cm the peak-to-total ratios lie within the range 0.75 to 0.80 for the 0.511-MeV photon. By accounting for attenuation by the light shield and reflector material of the side detectors and by assuming that one annihilation quantum is captured by each of the side detectors, the probability of capturing both of the quanta which escape from the center detector within the photopeak of the side detectors is given by

$$P_{j,k}[\text{pair capture}] = \left\{\exp\left[-\frac{1}{\sin\theta}\left(\mu_f x_s + \mu_r y_s\right)\right]\right\}^2 F^2 P_{j,k}[\text{interaction of } \overline{1}]\, P_{j,k}[\text{interaction of } \overline{2}] \tag{25}$$

where μ_f and μ_r are the respective attenuation coefficients for the light shield material and reflector material of the side detectors, x_s is the shield thickness, y_s is the reflector thickness, and F is the peak-to-total ratio for the side detectors for the 0.511-MeV photons.

By combining the probabilities for pair production, escape from the center detector, attenuation by the detector housings, and capture of pairs, and by summing over θ and φ, the total probability (or efficiency) of producing and capturing the annihilation quanta for an incident photon with energy E is given by

$$P[E] = P[\text{entrance}] \sum_{i=1}^{\frac{2R_S - I}{\Delta t}} \left\{ P_i[\text{pair production}] \sum_{j=0}^{\alpha_\theta} 2 \sum_{k=1}^{\frac{\alpha_\varphi}{2} - 1} P_{j,k}[\Delta\Omega]\, P_{j,k}[\text{escape}]\, P_{j,k}[\text{pair capture}] \right\} \tag{26}$$

The summation over i is terminated at

$$t = 2R_S - I \tag{27}$$

since for $t < 2R_S - I$, at least one photon of a pair would escape being captured by a side detector. The summation over k allows φ to vary from $\frac{-\pi}{2} - \Delta\varphi$ to $\frac{\pi}{2} - \Delta\varphi$ so that there will be no contribution for $\varphi = \frac{-\pi}{2}$ or for $\varphi = \frac{\pi}{2}$. The reason for this limitation is that the two side-detector crystals are separated by approximately 0.6 cm. With the proper choice of α_φ, the loss in available solid angle for capturing the pairs may be taken into account.

RESPONSE OF THE SPECTROMETER

As stated previously, in order to use a spectrometer such as described in this report, it is necessary to know the response of the spectrometer to monoenergetic photons over the energy range of interest; that is, it is necessary to know the pulse-height distributions produced by photons with energy between E and $E + \Delta E$ over the entire energy range of interest. If a set of monoenergetic sources existed with energies in each increment ΔE, experimental measurements could be made to furnish the necessary response. Since no complete set exists over the energy range from 1.0 MeV to 10.0 MeV, the response was calculated by using one available source and the predicted efficiencies for the other energies. The simplicity of the pulse-height distribution taken with the three-crystal pair spectrometer for a monoenergetic photon source greatly simplifies this task.

As shown in figure 3(b), the pulse-height distribution for the 4.43-MeV photons consists essentially of the sum of a Gaussian shaped peak and a triangular-shaped low-energy tail. In order to calculate the response of the detector to other energies, essentially the same shapes were assumed; however, the following criteria were used:

(1) The full widths at half maximum of the Gaussian shaped peaks were made proportional to the square root of E - 1.022 MeV

(2) The areas under the triangular-shaped regions were made proportional to E - 1.022 MeV

(3) The total area under each pulse-height distribution was normalized to the total efficiency of the detector at the particular photon energy

The first criterion is based on the usual convention that the resolution of a scintillation detector is inversely proportional to the square root of the energy deposited in the detector, which for a pair-production process is E - 1.022 MeV. Consequently, the

actual width would be proportional to the square root of the energy deposited. The second criterion arises from the use of the approximation that the fraction of electron or positron energy converted into bremsstrahlung in a thick target is proportional to the incident energy. (See ref. 6.) The constants of proportionality for the Gaussian widths and areas under the triangular-shaped tails were determined from the measured 4.43-MeV-photon pulse-height distribution. This procedure was programed, and a 63 by 63 response matrix was computed.

UNFOLDING OF THE PHOTON SPECTRA

The measured pulse-height distribution taken with a spectrometer, as described in this report, of a multienergetic photon source or a continuous distribution of photon energies is a result of summing the pulse-height distributions produced by a number of monoenergetic photons. Because of the finite resolution of the spectrometer and the bremsstrahlung and electron losses which are dependent on the incident photon energy, the instrument response is nonunique; and some method of analyzing, or unfolding, the pulse-height distributions must be used to give the actual incident photon spectra.

If an incident photon spectrum is represented by a column matrix $\underline{N}$ and if the response of a spectrometer is represented by a matrix $\underline{B}$, the pulse-height distribution $\underline{M}$ produced by the spectrometer is given by

$$\underline{M} = \underline{B}\,\underline{N} \tag{28}$$

The problem is then reduced to solving the matrix equation

$$\underline{N} = \underline{B}^{-1}\underline{M} \tag{29}$$

This straightforward approach has been found to yield poor results because inherent errors in the response matrix are magnified by the inversion process. (See ref. 7.) Therefore, the method used in the present report is the iterative method described in reference 4, which is discussed in some detail in the appendix. This iterative procedure has been shown to yield much better accuracy than the matrix inversion method. (See ref. 7.)

RESULTS AND DISCUSSION

The dimensions of the spectrometer are given in table I. The attenuation coefficients used for determining the spectrometer efficiency were obtained from reference 8 and are given in table II.

Equation (26) for the total probability of detection (or efficiency) has been programed for the digital computers at Langley Research Center, and the calculated efficiencies are given in figure 6 by the solid line drawn over the photon energy range from 1.022 MeV to 10.0 MeV. Below 1.5 MeV, the pair-production cross section for NaI is very small; therefore, experimental verification of the efficiency of the detectors at these low energies would require very long counting times and be subject to relatively large statistical errors.

The only readily available source of relatively high-energy (greater than 3 MeV) gamma rays was an americium-beryllium (Am-Be) neutron source which gives off a 4.43-MeV gamma ray. The activity of this source was calibrated by measuring the number of 4.43-MeV gamma rays in the photo peak of spectra taken with a 7.62-cm by 7.62-cm NaI scintillation detector. The efficiency and photofraction for the detector were obtained from reference 9. By using this source, the measured efficiency of the three-crystal pair spectrometer was found to be 7.9×10^{-3} as shown by the circular symbol in figure 6. The error bars indicate the combined possible error due to counting statistics for both the single-crystal detector and pair spectrometer and placing an uncertainty of ±10 percent on the data of reference 9. The square symbols shown in figure 6 are efficiency calculations found by using only simple pair-production attenuation, and neglecting geometrical considerations. Equation (26) then reduces to

$$P_g[E] = \epsilon \left\{ 1 - \exp\left[-\mu_g \left(2R_S - I \right) \right] \right\} \tag{30}$$

where μ_g is the pair-production attenuation coefficient at photon energy E, R_S is the radius of the side detectors, I is the indentation of the center crystal into the well, and ϵ is a normalization factor. The normalization factor was obtained by equating the calculated efficiency of the system from equation (26) at 5 MeV and equation (30). At 10 MeV the simple calculation differs by 13 percent from the calculations which include the specific geometry of the detector system. If a normalization point had been chosen with lower photon energy, the relative difference would be increased for the higher photon energies. If the spectrometer efficiency were experimentally measured with a calibrated source such as the Am-Be source with the 4.43-MeV gamma ray, the use of the simple calculation (eq. (30)) to obtain the efficiency at higher energies would cause an underestimation of at least 13 percent at 10 MeV.

After a Compton scattering, the scattered photon can possibly undergo a pair-production process. Calculations have been made to determine the error introduced by neglecting this type of multiple interaction. These calculations were made by finding the average energy of Compton scattered photons produced by 10.2-MeV and 6.6-MeV incident photons on NaI and by finding the average depth in the center detector of such Compton scatterings. The probability of having such an average scattering and then having the

scattered photon undergo a pair-production process in the remaining detector thickness was then computed. This probability was found to be 4.5 percent and 3.8 percent of the probability of having single pair-production processes at incident energies of 10.2 MeV and 6.6 MeV, respectively. These percentages should be an overestimation because no allowance was made for the Compton scattered photons being deflected from the incident direction.

The stripping approximation and the iterative unfolding procedure were programed for the Control Data series 6000 computer system at Langley Research Center, and a test case was run to check the convergence of the iterative procedure. A simulated bremsstrahlung spectrum was multiplied by the response matrix to yield a simulated pulse-height distribution. This simulated pulse-height distribution was stripped to yield the first approximation to the energy spectrum and then unfolded by the iterative procedure to yield the approximate bremsstrahlung energy spectrum. Table III gives the input energy spectrum, the simulated pulse-height spectrum, the stripped approximation, the first approximation as used in reference 4, and the iterative approximation to the energy spectrum after 201 iterations. As shown, the iterative approximation is within 1 percent except for photon energies of 10.35 MeV and 10.50 MeV. It can also be seen that the stripping procedure approximates the input much better than does the first approximation of reference 4. This improvement should greatly reduce the number of iterations necessary for good convergence.

The improvement obtained by using the iterative procedure rather than inverting the response matrix as in equation (29) can be seen immediately in figure 7, which shows the percent difference between the input spectra of table III and the unfolded spectra by both the iterative method and the matrix inversion method. The data points for the matrix inversion method are not shown for channels at which they did not differ from the iterative method sufficiently enough to be distinguished in the figure. The matrix inversion process is shown to exhibit oscillations about the input data, as mentioned in reference 7. These oscillations or instabilities generate errors as large as 30 percent. Although these oscillations for continuous spectra may be smoothed out, the direct inversion process is not well suited for spectra containing discrete energy peaks.

CONCLUDING REMARKS

An investigation has been made of the use of a three-crystal spectrometer for measurements of photon spectra. Calculations have been made of the efficiency and response of the spectrometer system for a photon energy range of 1.5 MeV to 10.0 MeV. An iterative spectrum-unfolding method has been modified to permit operation with a spectrometer system of low efficiency, such as the three-crystal spectrometer. The efficiency calculations appear to have good accuracy when compared with a limited amount of

experimental data and would appear to be an improvement on simple calculations which neglect the specific geometry of the system. The iterative unfolding technique has proved to yield errors which are insignificant in comparison with errors in either efficiency or response and has proved to be much superior to unfolding by the matrix inversion method.

Langley Research Center,
National Aeronautics and Space Administration,
Langley Station, Hampton, Va., May 19, 1969,
124-09-11-03-23.

APPENDIX

ITERATIVE ANALYSIS OF PHOTON SPECTRA

The method to be described and used to unfold the photon spectra is based on the iterative method described by Smith and Scofield in reference 4. The incident photon-energy spectrum is represented by a column matrix $\underline{N}$ in which each row element N_n represents the number of photons in an energy interval n. The measured pulse-height distribution is represented by a column matrix $\underline{M}$ in which each row element M_m represents the number of pulses in a pulse-height interval m. The response of the detector to some photon with energy in the interval n can be represented by a rectangular matrix $\underline{B}$ in which the elements B_{mn} of the nth column are the probabilities that a photon with energy in the nth energy interval will produce a count in the mth pulse-height interval. The problem of analyzing some measured pulse-height distribution is then reduced to finding the elements N_n where

$$\underline{M} = \underline{B}\,\underline{N} \tag{A1}$$

If equation (A1) is multiplied by the transpose of the response matrix, then

$$\underline{\tilde{B}}\,\underline{M} = \underline{\tilde{B}}\,\underline{B}\,\underline{N} \quad \text{or} \quad \underline{S} = \underline{C}\,\underline{N} \tag{A2}$$

where the matrices $\underline{S}$ and $\underline{C}$ are defined as

$$\underline{S} = \underline{\tilde{B}}\,\underline{M} \quad \text{and} \quad \underline{C} = \underline{\tilde{B}}\,\underline{B}$$

The matrix $\underline{C}$ is square and symmetric.

The iterative method of reference 4 consists of calculating a diagonal matrix $\underline{D}$ as follows:

$$\underline{N} = \underline{D}\,\underline{S} \tag{A3}$$

Since $\underline{D}$ is diagonal, $\underline{S}$ and $\underline{N}$ must be of the same order, and equation (A3) can be written

$$N_p = D_{pp}S_p \tag{A4}$$

where N_p are the elements of $\underline{N}$, S_p are the elements of $\underline{S}$, and D_{pp} are the diagonal elements of $\underline{D}$.

The elements of $\underline{D}$ can be found by

$$D_{pp} = \frac{N_p}{S_p} \tag{A5}$$

where the off-diagonal elements, of course, are zero. The iterative scheme consists of the following steps:

(1) A set of values for the energy spectrum N^q is approximated, where q represents the number of iterations, and $q = 1$ for steps (1) through (4)

(2) Approximate values for the $\underline{S}$ matrix are calculated by

$$\underline{S}^q = \underline{C}\,\underline{N}^q \qquad (q = 1) \tag{A6}$$

(3) An approximate set of diagonal elements for $\underline{D}$ is computed by

$$D_{pp}^q = \frac{N_p^q}{S_p^q} \qquad (q = 1) \tag{A7}$$

(4) The sum of the squares of the differences of the elements of $\underline{S} = \underline{B}\underline{M}$ and $\underline{S}^q$ are computed by

$$T^q = \left(S_p - S_p^q\right)^2 \qquad (q = 1) \tag{A8}$$

(5) The next approximation for $\underline{N}^q$ is computed by

$$\underline{N}^{q+1} = \underline{D}^q \underline{S} \tag{A9}$$

(6) The next approximation for $\underline{S}$ is computed by

$$\underline{S}^{q+1} = \underline{C}\,\underline{N}^{q+1} \tag{A10}$$

(7) The next approximation for $\underline{D}$ is computed by

$$D_{pp}^{q+1} = \frac{N_p^{q+1}}{S_p^{q+1}} \tag{A11}$$

(8) The test for the convergence of $\underline{S}^{q+1}$ is made by

$$T^{q+1} = \left(S_p - S_p^{q+1}\right)^2 \tag{A12}$$

(9) Steps (5) to (8) are repeated until

$$T^{q-1} - T^q < T^q - T^{q+1} \tag{A13}$$

or until q reaches a predetermined value

The $\underline{N}^q$ computed when either of the conditions of (9) is met is considered to be the incident photon-energy spectrum. A thorough discussion of the convergence and uniqueness of the solution is given in reference 7.

The remaining problem to be solved is to make a reasonable first approximation for $\underline{N}$. In reference 4 this approximation was accomplished for the case of a single-crystal NaI detector by letting

$$\underline{N}^1 = \underline{S} = \underline{\tilde{B}}\,\underline{M} \tag{A14}$$

However, the detection efficiency of the three-crystal pair spectrometer is several orders of magnitude less than that of a single-crystal NaI spectrometer; therefore, the use of equation (A14) would result in a severe underestimation for the first approximation of the iterative procedure. Because of this underestimation a somewhat different approach is used herein.

A method of stripping the measured pulse-height distribution into a photon-energy spectrum was used for the first approximation for $\underline{N}$ for the three-crystal spectrometer. Because of the narrow Gaussian peaks in the response matrix, the last element of the pulse-height distribution M_u is mainly a result of the last two elements of the photon spectra N_v and N_{v-1}. Consequently,

$$M_u \approx B_{u,v}N_v + B_{u,v-1}N_{v-1} \tag{A15}$$

If N_v is approximately equal to N_{v-1}, then

$$N_v^1 \approx \frac{M_u}{B_{u,v} + B_{u,v-1}} \tag{A16}$$

The pulse-height distribution can be stripped by subtracting the contribution to each element of the pulse-height distribution by the number of incident photons with energy in the vth energy interval from the elements of $\underline{M}$:

$$M_m^1 \approx M_m - B_{m,v}N_v^1 \tag{A17}$$

Similarly,

$$N_{v-1}^1 \approx \frac{M_{v-1}^1}{B_{u-1,v-1} + B_{u-1,v-2}} \tag{A18}$$

By continuing these steps, a general recursion relation can be found so that the number of photons in the nth energy interval can be approximated by

$$N_n^1 \approx \frac{M_n - \sum_{m=n+1}^{u} B_{n,m}N_m^1}{B_{n,n} + B_{n,n-1}} \tag{A19}$$

where $n = v,\ v-1,\ v-2, \ldots 1$ and equation (A16) holds if $n = v$.

REFERENCES

1. Bent, R. D.; and Kruse, T. H.: Gamma-Emitting States in 0^{16} Below 12 Mev. Phys. Rev. Second ser., vol. 108, no. 3, Nov. 1, 1957, pp. 802-809.

2. Alburger, D. E.; and Toppel, B. J.: Radioactive Decays of Rh^{106} and Ag^{106}. Phys. Rev., Second ser., vol. 100, no. 5, Dec. 1, 1955, pp. 1357-1363.

3. Treado, P. A.; and Chagnon, P. R.: Neutron Capture Gamma-Ray Spectra of the Nickel Isotopes. Phys. Rev., Second Ser., vol. 121, no. 6, Mar. 15, 1961, pp. 1734-1739.

4. Smith, Charles V.; and Scofield, Norman E.: A Computer Program for Unfolding Pulse-Height Distributions. USNRDL-TR-829, U.S. Navy, May 17, 1965. (Available from DDC as AD 463 254.)

5. Weitkamp, C.: Monte-Carlo Calculation of Photofractions and Intrinsic Efficiencies of Cylindrical NaI(Tl) Scintillation Detectors. Nucl. Instrum. Methods, vol. 23, no. 1, May 1963, pp. 13-18.

6. Evans, Robley D.: The Atomic Nucleus. McGraw-Hill Book Co., Inc., c.1955, pp. 614-617.

7. Gold, R.: An Iterative Solution of the Matrix Representation of Detection Systems. RED-EPM #114, Argonne Nat. Lab., Jan. 8, 1963.

8. Davisson, C. M.: Gamma-Ray Attenuation Coefficients. Alpha-, Beta-, and Gamma-Ray Spectroscopy, volume 1, Kai Siegbahn, ed., North-Holland Pub. Co. (Amsterdam), 1966, pp. 827-843.

9. Vegors, Stanley H., Jr.; Marsden, Louis L.; and Heath, R. L.: Calculated Efficiencies of Cylindrical Radiation Detectors. AEC Res. and Dev. Rep. IDO-16370, U.S. At. Energy Comm., Sept. 1, 1958.

TABLE I.- SPECTROMETER DIMENSIONS

Center crystal:	
Length	10.16 cm
Radius	2.06 cm
Light-shield thickness	0.04 cm
Reflector thickness	0.28 cm
Side crystals:	
Height	7.62 cm
Radius	6.35 cm
Light-shield thickness	0.05 cm
Reflector thickness	0.11 cm
Radius of groove	2.70 cm
Indentation of center detector into well	2.86 cm

TABLE II.- ATTENUATION COEFFICIENTS

Photon energy, MeV	Attenuation coefficients, cm^{-1}				
	NaI total	NaI pair production	Al total	Fe total	Al_2O_3 total
0.5	0.350	0.0000	0.228	0.659	0.300
1.0	.215	.0000	.166	.469	.219
1.5	.172	.0027	.135	.381	.178
2.0	.151	.0090	.117	.333	.152
3.0	.134	.0234	.095	.283	.126
4.0	.129	.0369	.084	.259	.109
5.0	.127	.0482	.076	.246	.098
6.0	.128	.0577	.072	.239	.088
8.0	.130	.0731	.065	.233	.082
10.0	.135	.0894	.062	.232	.077
15.0	.147	.1115	.059	.240	.070

TABLE III.- UNFOLDING-PROCEDURE TEST CASE

Photon energy, MeV	Input energy spectrum, photons/MeV	Simulated spectrum, counts/channel	Stripped approximation, photons/MeV	First approximation (ref. 4), photons/MeV	Iterative unfolding, photons/MeV
1.20	4 400 000	1163.0	4 390 200	0.16210	4 397 300
1.35	3 200 000	1801.0	3 190 800	0.47111	3 199 900
1.50	2 700 000	2380.0	2 690 500	0.93552	2 700 900
1.65	2 100 000	3037.0	2 090 600	2.0710	2 099 400
1.80	1 900 000	3680.0	1 892 300	3.6045	1 900 600
1.95	1 750 000	4225.0	1 742 700	5.4470	1 750 200
2.10	1 620 000	4697.0	1 613 200	7.6392	1 619 700
2.25	1 500 000	5095.0	1 495 600	10.082	1 500 100
2.40	1 500 000	5582.0	1 490 400	12.971	1 500 000
2.55	1 450 000	5935.0	1 443 400	15.951	1 449 800
2.70	1 400 000	6219.0	1 393 900	19.029	1 399 800
2.85	1 350 000	6443.0	1 344 500	22.176	1 349 800
3.00	1 300 000	6609.0	1 295 600	25.349	1 300 200
3.15	1 260 000	6717.0	1 255 100	28.179	1 260 000
3.30	1 230 000	6794.0	1 223 300	30.954	1 229 800
3.45	1 190 000	6806.0	1 185 100	33.571	1 189 900
3.60	1 140 000	6751.0	1 137 800	35.975	1 139 900
3.75	1 090 000	6653.0	1 088 700	38.185	1 090 000
3.90	1 040 000	6526.0	1 040 400	40.232	1 040 000
4.00	1 000 000	6385.0	1 000 400	41.981	1 000 200
4.20	970 000	6212.0	966 880	43.212	969 590
4.35	920 000	5980.0	925 120	44.122	920 630
4.50	880 000	5697.0	879 570	44.658	879 280
4.65	800 000	5342.0	814 870	44.834	800 890
4.80	750 000	5008.0	758 780	44.804	749 230
4.95	700 000	4661.0	707 880	44.510	700 820
5.10	630 000	4241.0	643 860	43.602	628 980
5.25	550 000	3789.0	571 640	42.263	551 370
5.40	490 000	3349.0	504 310	40.717	488 680
5.55	410 000	2893.0	431 380	38.999	411 210
5.70	333 000	2455.0	356 130	37.243	332 250
5.85	273 000	2093.0	292 760	35.657	272 830
6.00	230 000	1814.0	245 510	34.331	230 920
6.15	200 000	1593.0	210 330	33.068	199 000
6.30	170 000	1409.0	181 290	31.984	170 930
6.45	150 000	1261.0	158 370	31.050	149 810
6.60	135 000	1142.0	140 990	30.239	134 440
6.75	120 000	1041.0	126 650	29.518	120 840
6.90	110 000	954.0	114 750	28.862	109 590
7.05	100 000	877.0	104 620	28.255	100 020
7.20	91 000	807.0	95 225	27.687	90 784
7.35	83 000	746.0	87 344	27.157	83 288
7.50	77 000	692.0	80 575	26.663	76 982
7.65	72 000	644.0	74 771	26.201	71 396
7.80	66 000	601.0	69 739	25.764	66 699
7.95	63 000	562.0	65 633	25.348	62 862
8.10	59 000	524.0	61 393	24.949	58 548
8.25	54 000	489.0	57 453	24.567	54 514
8.40	52 000	458.0	54 068	24.204	51 442
8.55	49 000	431.0	51 720	23.859	49 317
8.70	47 000	405.0	49 122	23.532	46 731
8.85	45 000	383.0	47 392	23.220	45 073
9.00	44 000	363.0	46 244	22.920	44 144
9.15	43 000	343.0	45 096	22.627	42 981
9.30	42 000	323.0	43 947	22.338	41 623
9.45	40 000	303.0	42 790	22.050	40 266
9.60	39 000	283.0	41 594	21.763	38 934
9.75	38 000	263.0	40 474	21.475	37 768
9.90	36 000	242.0	39 288	21.182	36 572
10.05	35 000	219.0	37 770	20.832	34 778
10.20	32 000	193.0	35 509	20.369	31 816
10.35	30 000	159.0	33 422	19.852	28 998
10.50	28 000	105.0	34 211	19.274	29 562

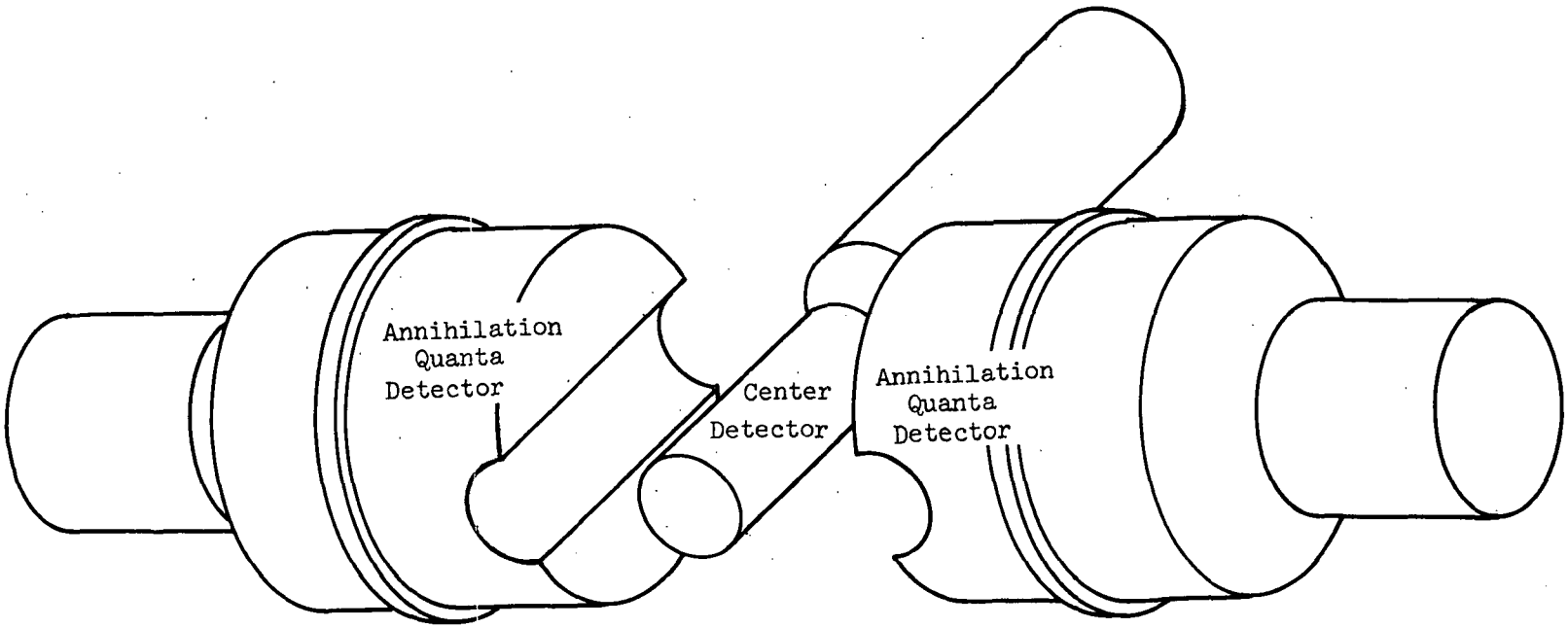

Figure 1.- Three-crystal pair spectrometer.

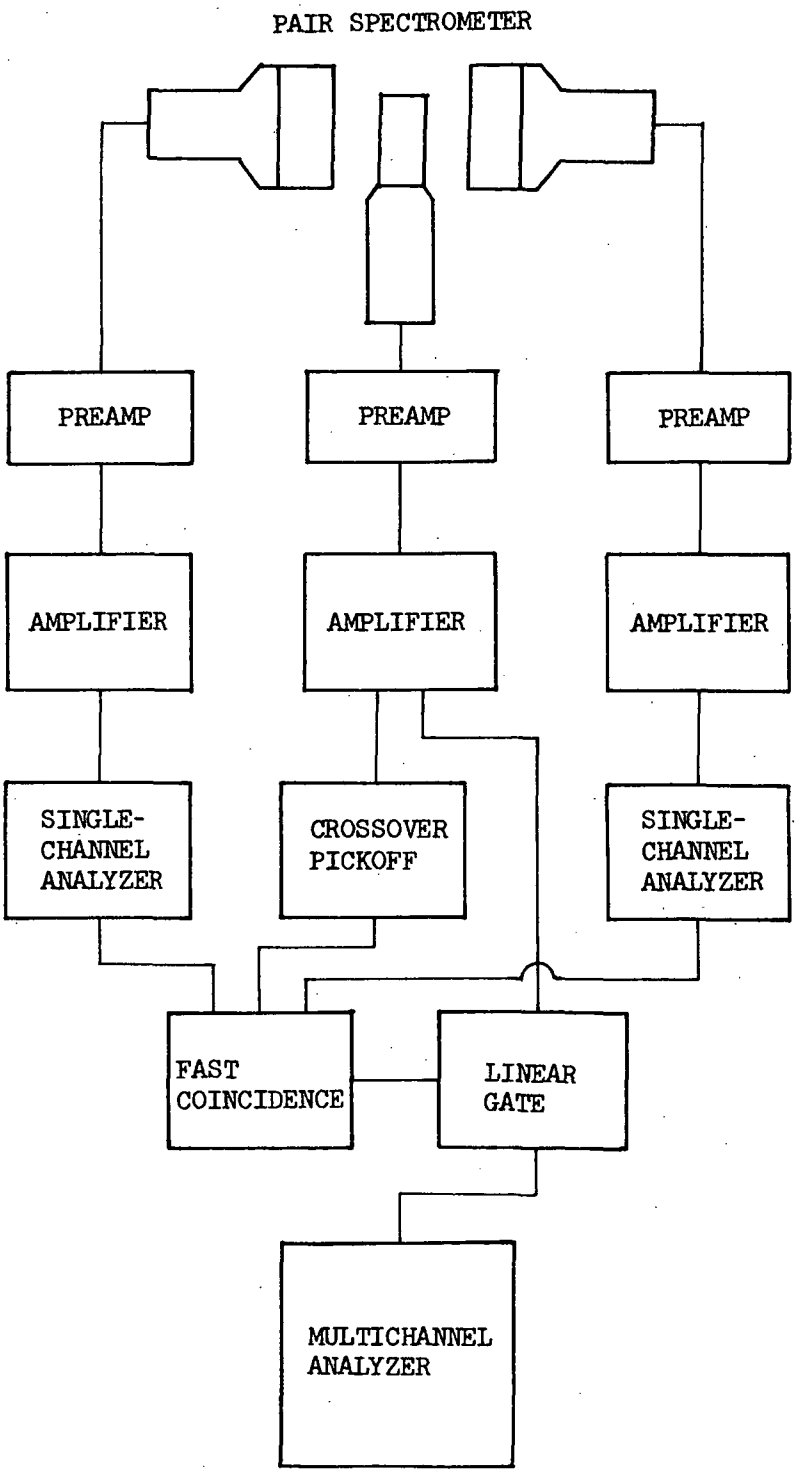

Figure 2.- Spectrometer electronics diagram.

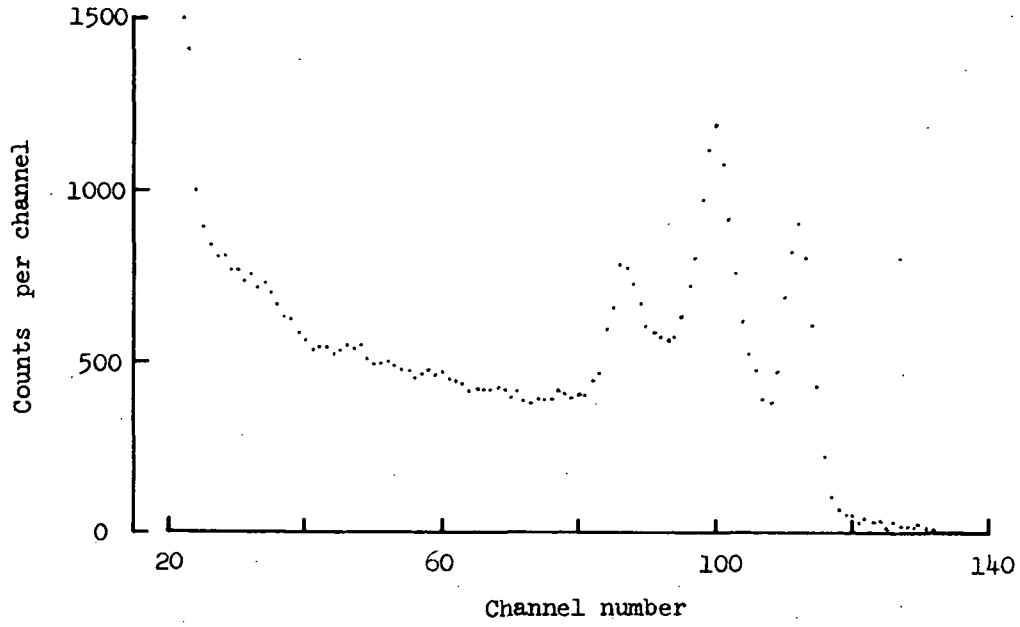

(a) 7.62-cm by 7.62-cm single-crystal NaI detector.

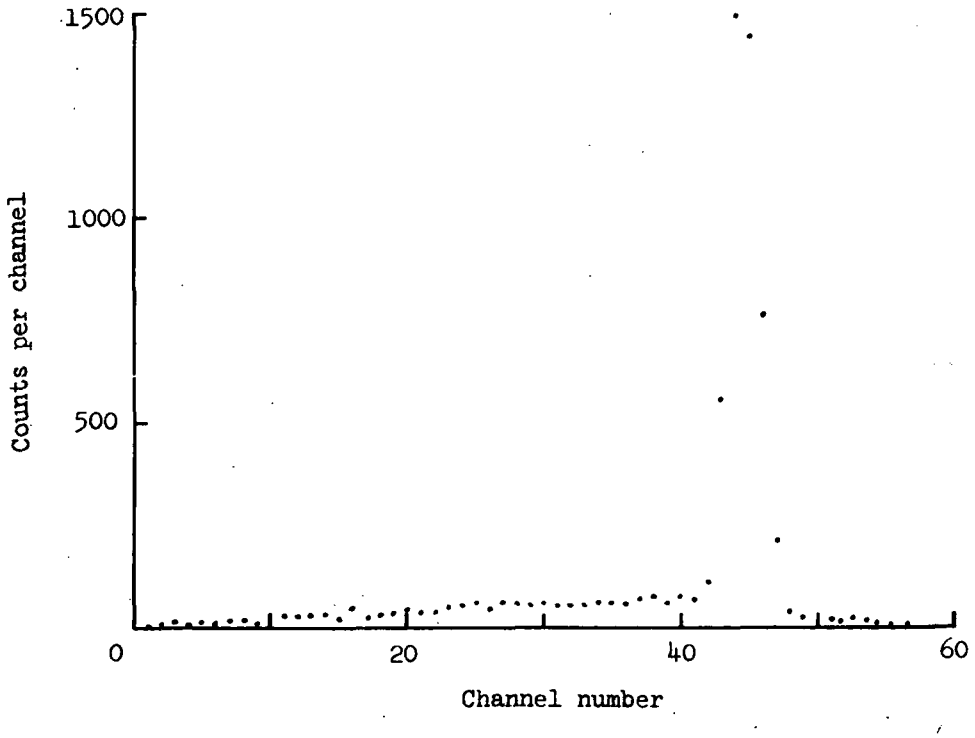

(b) Three-crystal spectrometer.

Figure 3.- 4.43-MeV gamma-ray pulse-height distributions.

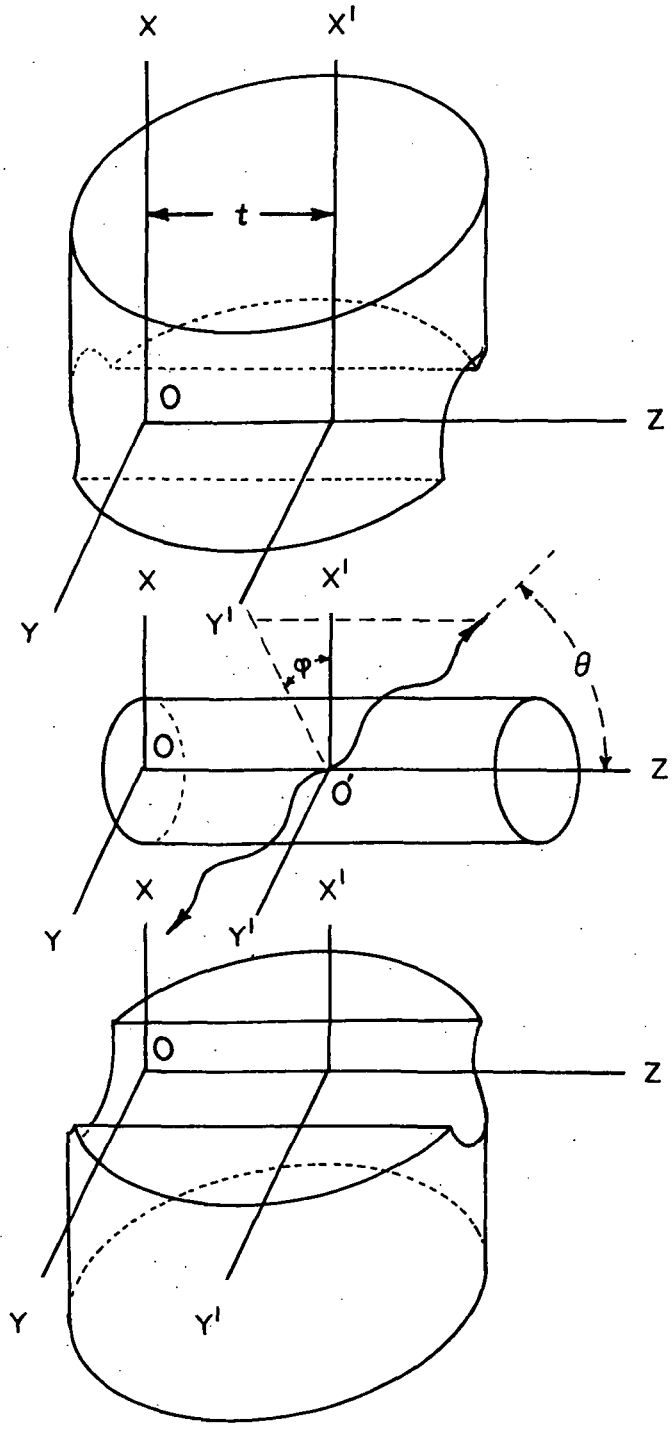

Figure 4.- Spectrometer geometry.

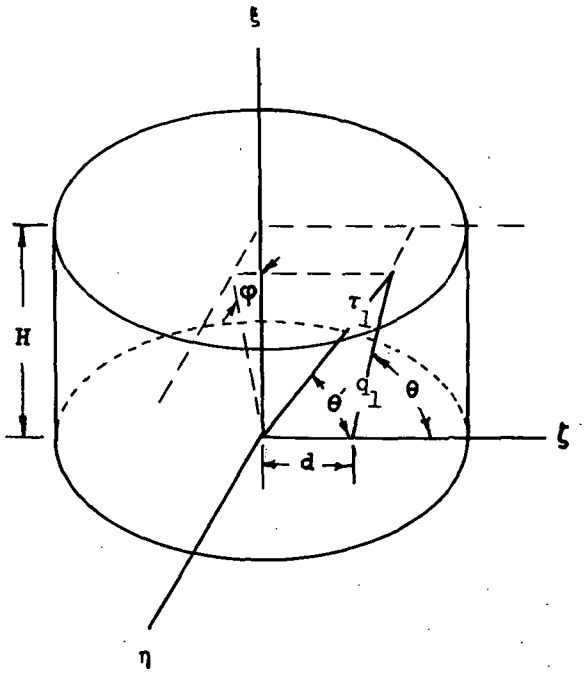

(a) Distance to crystal face.

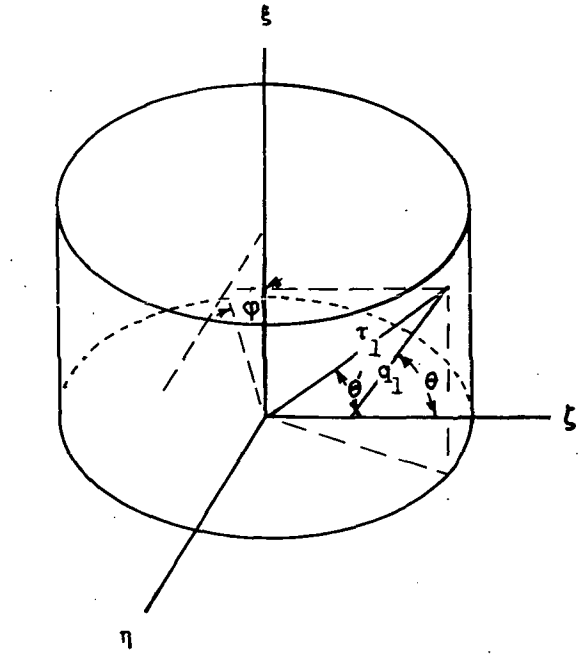

(b) Distance to crystal side.

Figure 5.- Geometry for annihilation pair detection.

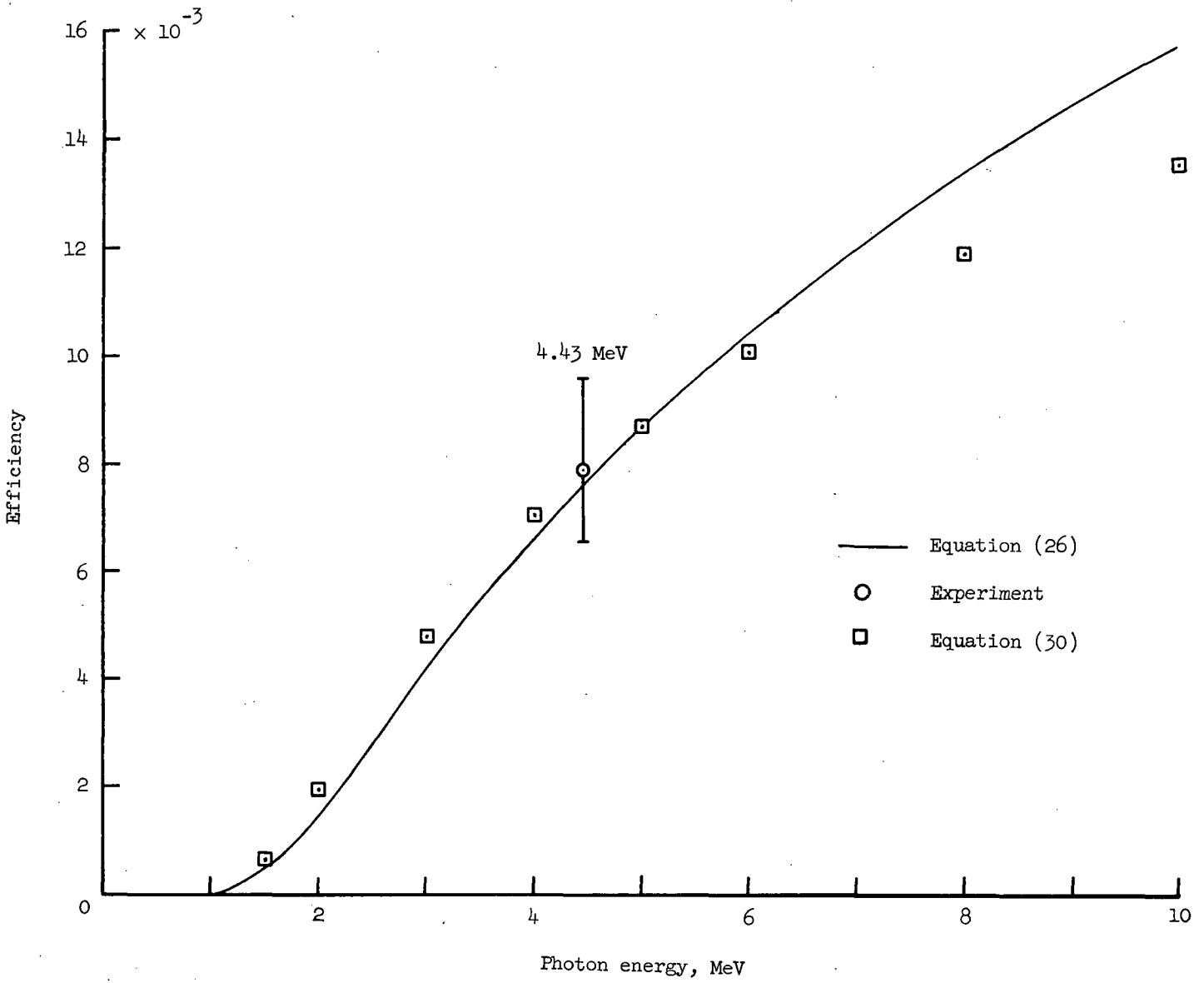

Figure 6.- Efficiency of three-crystal pair spectrometer.

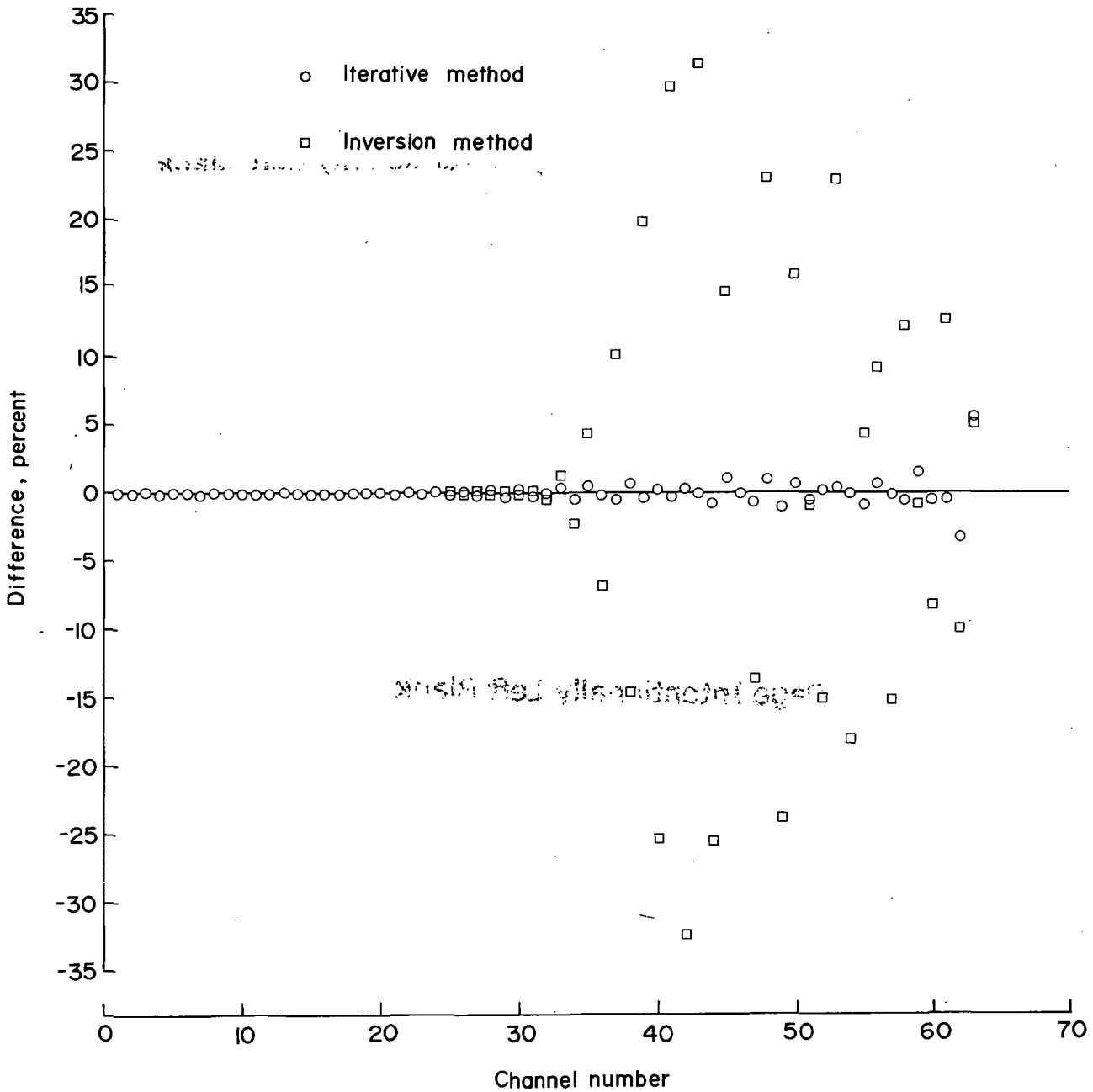

Figure 7.- Difference between input spectrum and unfolded spectra.

Page Intentionally Left Blank

"The aeronautical and space activities of the United States shall be conducted so as to contribute . . . to the expansion of human knowledge of phenomena in the atmosphere and space. The Administration shall provide for the widest practicable and appropriate dissemination of information concerning its activities and the results thereof."

—NATIONAL AERONAUTICS AND SPACE ACT OF 1958

NASA SCIENTIFIC AND TECHNICAL PUBLICATIONS

TECHNICAL REPORTS: Scientific and technical information considered important, complete, and a lasting contribution to existing knowledge.

TECHNICAL NOTES: Information less broad in scope but nevertheless of importance as a contribution to existing knowledge.

TECHNICAL MEMORANDUMS: Information receiving limited distribution because of preliminary data, security classification, or other reasons.

CONTRACTOR REPORTS: Scientific and technical information generated under a NASA contract or grant and considered an important contribution to existing knowledge.

TECHNICAL TRANSLATIONS: Information published in a foreign language considered to merit NASA distribution in English.

SPECIAL PUBLICATIONS: Information derived from or of value to NASA activities. Publications include conference proceedings, monographs, data compilations, handbooks, sourcebooks, and special bibliographies.

TECHNOLOGY UTILIZATION PUBLICATIONS: Information on technology used by NASA that may be of particular interest in commercial and other non-aerospace applications. Publications include Tech Briefs, Technology Utilization Reports and Notes, and Technology Surveys.

Details on the availability of these publications may be obtained from:

SCIENTIFIC AND TECHNICAL INFORMATION DIVISION

NATIONAL AERONAUTICS AND SPACE ADMINISTRATION

Washington, D.C. 20546